Cite this paper: Vietnam J. Chem., **2023**, *61(2)*, 210-219
DOI: 10.1002/vjch.202200125

Research article

Synthesis of metal organic framework based on Cu and benzene-1,3,5-tricarboxylic acid (H_3BTC) by potentiodynamic method for CO_2 adsorption

Nguyen Thu Phuong[1], Do Thi Hai[2], Thomas Doneux[3], Nguyen Hong Nam[4*], Dinh Thi Mai Thanh[1,4*]

[1] *Institute for Tropical Technology, Vietnam Academy of Science and Technology, 18 Hoang Quoc Viet, Cau Giay, Hanoi 10000, Viet Nam*

[2]*Hanoi University of Mining and Geology, 18 Pho Vien, Duc Thang, Bac Tu Liem, Hanoi 10000, Viet Nam*

[3]*Chemistry at Surfaces, Interfaces and Nanostructure (ChemSIN), Faculté des Sciences, Université Libre de Bruxelles, Boulevard du Triomphe, 2, CP 255, B-1050 Bruxelles, Belgium*

[4]*University of Science and Technology of Hanoi, Vietnam Academy of Science and Technology, 18 Hoang Quoc Viet, Cau Giay, Hanoi 10000, Viet Nam*

Submitted July 4, 2022, Revised August 21, 2022; Accepted October 25, 2022

Abstract

Practical CO_2 adsorption processes require adsorbents that can be easily and quickly synthesized at a reasonable cost, while maintaining a significant adsorption performance. In this research, a metal organic framework based on Cu and H_3BTC was synthesized by the potentiodynamic method. Results showed that the nature of the solvent strongly affected the phase structure, morphology and specific surface area of the obtained material. In methanol, a mixture of 1D structure Cu-BTC (catena-triaqua μ-[1,3,5-benzenetricarboxylato]-copper (II) corresponding to the formula $[Cu(BTC)(H_2O)_3)]_n$ and micropillars structure $Cu(BTC).3H_2O$ was obtained. The 1D structure Cu-BTC had a plate shape and a small specific surface area of 21 m^2/g. In ethanol, the 3D structure Cu-BTC ($Cu_3(BTC)_2$) was successfully synthesized. The obtained material has a cubic shape of size from 50 nm to 500 nm and a much better specific surface area of 620 m^2/g. The 3D structure Cu-BTC offered a high CO_2 adsorption capacity of 3.6 mmol/g at standard conditions, and 1.6 mmol/g at more realistic conditions.

Keywords. Cu-BTC, crystal structure, metal organic framework, CO_2 adsorption.

1. INTRODUCTION

The current concentration of CO_2 in the atmosphere, the most significant contributor to global warming, is 420 ppm, higher than about 50 % of the beginning of the industrial revolution in 1750.[1] Meanwhile, the "acceptable" level of CO_2 concentration should be limited at below 570 ppm in 2100 to keep the rise of global temperature of less than 2 °C.[2] To achieve this goal, big efforts should be done to reduce atmospheric CO_2 concentration. The application of new and efficient adsorbents for CO_2 capture is one of the promising solutions for this issue.[3] In stationary point sources such as power plants or cement kilns, CO_2 emissions can be greatly reduced by using CO_2 capture technologies.[4] In this context, the metal-organic framework (MOF) is attracting more and more attention from researchers and developers as a new group of materials for CO_2 adsorption.

MOFs may have a 1D, 2D or 3D structure and are formed from metallic ions or clusters with organic ligands. It has many remarkable properties such as high porosity, low density, high adsorption ability, catalysis ability and high specific surface area, leading to applications in various fields such as gas separation and storage, gas purification, electrocatalysis, super capacity, electrode material for battery, pollutant removal and water purification.[5-16] MOF can be synthesized by different methods, e.g. mechanochemical method, solvothermal method, chemical method, microwave method, and electrochemical method.[5,10,15,17-26] Electrochemical is considered a promising method because it allows synthesizing a high quantity of pure materials for a short duration in a controlled way.[27] Besides galvanostatic or potentiostatic, potentiodynamic synthesis is mostly used to synthesize MOF thanks to the simplicity of the process.[24]

Many factors can affect the morphology, structure and the properties of the synthesized material, such as the nature of the organic ligand or metallic ion, solvent, temperature, pH, synthesis method, and synthesis time.[21,28-30] The research to determine suitable conditions to synthesize MOF for practical applications still attracts lots of scientists. By changing the ligands or metallic ions, the porosity of the material can be modified to obtain a new structure that allows high selective adsorption abilities. Metallic ions of the A, IB or IVB groups are often used, such as Ni, Cu, or Co, particularly Cu because it is a common metal with lots of applications.[28,31] The most common ligands are carboxylates, phosphonates, sulfonates and N-heterocyclic compounds such as pyridine and imidazole.

$Cu_3(BTC)_2$ (MOF-199 or HKUST-1), formed from Cu and H_3BTC: benzene-1,3,5-tricarboxylic acid is one of the most studied MOF. It was first reported by Williams *et al.* in 1999.[32] In 1999, $Cu_3(BTC)_2$ and MOF-5 were synthesized and they are two types of MOFs that were researched extensively.[32] In 2017, the group of K. Domke reported on the adsorption of trimesic acid on Cu in ethanol. Cyclic voltammetric and Raman spectroscopic data indicate that a 2D adsorbate layer is formed at 0 V vs Cu. At higher coverages a multilayer of flat lying molecules is formed. When the potential is made more positive, a 3D MOF is produced due to the oxidation of the copper surface, as expected.[33]

This paper reported the synthesis of MOF based on Cu and H_3BTC by potentiodynamic method, with emphasis on the effect of the solvent's nature on the morphology, structure and specific surface area of the obtained material. The CO_2 adsorption performance of the obtained MOF was also assessed.

2. MATERIALS AND METHODS

2.1. MOF synthesis procedure

As the E_{OCP} of Cu electrode in the electrolyte was about 0 V/SCE and the maximum potential of Autolab device is 10 V, the Cu-BTC material was synthesized by the potentiodynamic method from 0-10 V/SCE and a scan rate of 5 mV/s in an electrochemical cell with 3 electrodes. The 3-electrode cell includes a saturated calomel reference electrode (SCE), a working electrode with a limited area of 10 cm^2 and a counter electrode (Cu 99.61 %, 20×50×3 mm in size). The Cu electrode surface was treated with abrasive paper, rinsed with distilled water and solvent before each measurement. Electrochemical experiments were performed on an Autolab device.

Two different types of 80 mL solution were applied parallelly for the synthesis: (SS1) methanol + 0.05 M H_3BTC + 0.05 M $NaNO_3$ and (SS2) ethanol + 0.05 M H_3BTC + 0.05 M $NaNO_3$. In which: H_3BTC ($C_9H_6O_6$), M = 210.14 g/mol, Merck, 95 % purity. Methanol, ethanol and $NaNO_3$ are pure chemical of China.

2.2. Analysis of MOF properties

The surface functional groups of the synthesized Cu-BTC were determined by a FT-IR NEXUS 6700 (Nicolet) from 400-3000 cm^{-1}. The morphology was examined by a SEM S4800 (Hitachi). The total and micropore specific surface areas were determined by the BET and t-plot methods using Micromeritics ASAP 2060. Data in the relative pressure (p/p_0) range from 0.025 to 0.30 were used to determine the surface area by the BET equation: $\frac{1}{X[(\frac{P}{P_0})-1]} = \frac{1}{X_m C} + \frac{C-1}{X_m C}(\frac{P}{P_0})$, as mentioned in previous studies.[34-36] Here, X represents the weight of nitrogen adsorbed at a given p/p_0, X_m represents the volume of gas adsorbed at standard temperature and pressure, and C is constant. The graph of the BET equation was linear with a positive slope of 0.207 g/cm^3 STP and a fitting coefficient of 0.999 was obtained in our measurements. From the XRD measurement (Siemens D5000 of Bruker - Germany), the distance between crystal planes d and the phase structure of Cu-BTC can be determined. While the 1D structure Cu-BTC has monoclinic structure,[37] the 3D structure Cu-BTC has faced-centered cubic structure with $a = b = c$ and $\alpha = \beta = \gamma = 90^o$.[10,38] From the Miller index (hkl) of the 3D structure Cu-BTC, the lattice parameter a can be determined following the equation: $d = \frac{a}{\sqrt{h^2+k^2+l^2}}$ (*).

2.3. CO_2 adsorption procedure

The CO_2 adsorption capacity of the sample was measured at standard conditions (25 °C, 100 % CO_2) and more realistic conditions (40 °C, 15 % CO_2 in N_2) using a Macro-thermogravimetric system, designed by the Centre de Coopération Internationale en Recherche Agronomique pour le Développement (CIRAD) and the University of Science and Technology of Hanoi (USTH) (figure 1).

The reactor consists of a 7.5-cm ceramic tube (1)

placed inside a Carbolite electrical furnace (2). The atmosphere can be generated by injecting desired gases (CO_2 or N_2) through a 2m-coiled pre-heater (3). For each experiment, the sample placed in the holder (4) is lifted to the center of the reactor. The mass loss is continuously weighed by a weight scale (5) and recorded to a computer. Meanwhile, an extractor (6) extracts the flue gas out of the system. The dried sample was exposed under a CO_2 gas flow of 3 L/min at different concentrations. When a stabilized uptake mass was obtained, the CO_2 flow was switched to pure N_2 to regenerate the sample. The CO_2 adsorption performance calculated as follows:

$$P_{CO_2}(\%) = \frac{m_f - m_i}{m_i} x\ 100$$

where m_i and m_f are the initial and final mass of the material before and after adsorption, respectively.

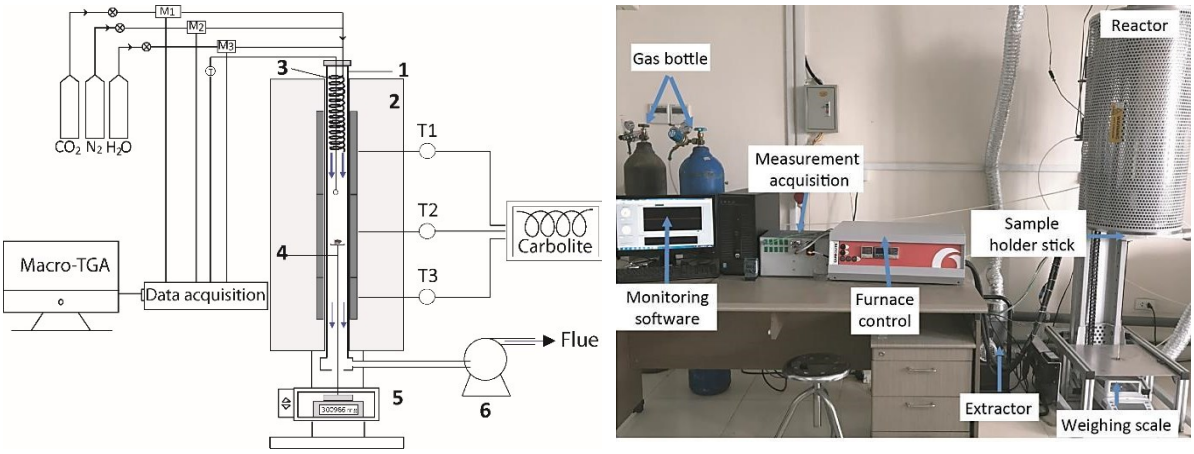

(a) (b)

Figure 1: The macro-thermogravimetric reactor: (a) diagram and (b) real setup

3. RESULTS AND DISCUSSION

3.1. Characteristics of the synthesized material

Figure 2 presents the value of the current when varying the potential from 0 to 10 V/SCE (scan rate 5 mV/s) at the Cu working electrode in SS1 and SS2 solutions. In ethanol, the response current was very low. At E = 10 V/SCE, the anodic current intensity was 0.05 A. In methanol, the current was markedly increased with the potential and at E = 10 V/SCE, an anodic current of 0.35 A was reached. A higher anodic current generally results in a faster process and this is thus expected to be more favorable for the production of the material. This result can be explained by the higher polarization - expressed by the dielectric coefficient - of methanol (having a value of 33) compared to that of ethanol (having a value of 24.55). Moreover, the structure of ethanol molecules is more voluminous than that of methanol. The $-C_2H_5$ group is bigger and thus can push electrons stronger than the $–CH_3$ group, leading to the higher polarization of O-H bond in methanol than in ethanol. Therefore, the solvation ability of $NaNO_3$ in methanol is much better compared to that in ethanol, leading a higher conductivity of the solution. The IR spectra of the H_3BTC and the synthesized Cu-BTCs in methanol and ethanol are shown in figure 3. For H_3BTC, the bands at 1710, 1180 and 1275 cm^{-1} could be attributed to the C=O, C-O stretching vibration and the bending vibration of O-H of the carboxylic acid group. The symmetric and antisymmetric stretching of O-C=O group was observed in the range 1380-1620 cm^{-1}. The broad band observed in the 2500-3300 cm^{-1} region corresponded to the O-H stretching of the carboxylic group. For Cu-BTC, the peaks at 1709, 1183, 1245 cm^{-1} and in the range 1376-1630 cm^{-1} could be attributed to the stretching vibrations $\nu_{C=O}$ and ν_{C-O}, the bending vibration of O-H, the symmetric and the antisymmetric stretching of O-C=O group, respectively. The broad band corresponding to the O-H stretching of the carboxylic groups is shifted to the 3100-3600 cm^{-1} region, indicating the presence of loosely bound water molecules in Cu-BTC (table 1).[5,17,38-40] From the high intensity of peak at 1275 cm^{-1} in H_3BTC (corresponding to the bending vibration of O-H of the carboxylic acid group) to the lower intensity in Cu-BTC synthesized in SS1 (at 1245 cm^{-1}) and we cannot observe this peak in SS2, it can be concluded that the sample obtained from SS1 still have acid groups and in SS2 all H_3BTC was fully deprotonated. A similar phenomenon is also observed in the broad band from 2500-3300 cm^{-1} or peak at 2553 cm^{-1} (O-H stretching of the carboxylic group). This result will be confirmed by the XRD analysis in the next part.

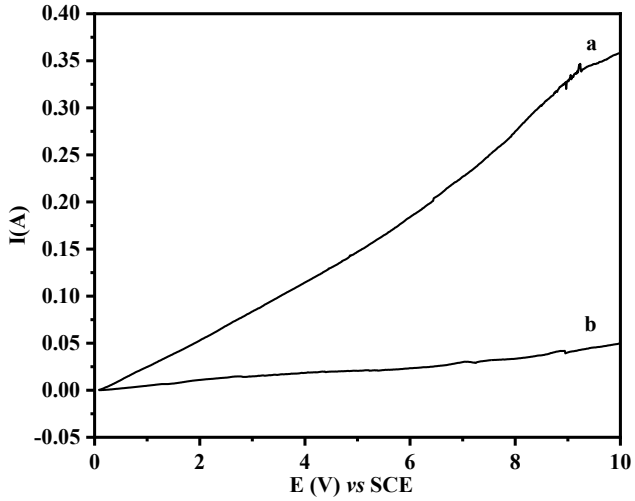

Figure 2: Current as a function of potential for the potentiodynamic synthesis process (v = 5 mV/s) of Cu-BTC in SS1 (a) and SS2 (b)

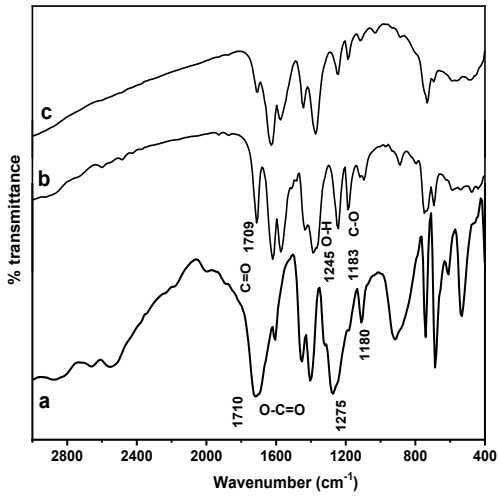

Figure 3: IR spectra of H_3BTC (a) and Cu-BTC synthesized by the potentiodynamic method in SS1 (b) and SS2 (c)

Table 1: Vibration groups of H_3BTC and CuBTC (wavenumbers are expressed in cm^{-1}).

Vibration group	$\nu_{C=O}$	ν_{C-O}	$\nu_{O-H\ bonding}$	$\nu_{O-C=O}$	$\nu_{O-H\ stretching}$
H_3BTC	1710	1180	1275	1380-1620	2553 (2500-3300)
Cu-BTC[17]	1710	1193	1232	1380-1620	
Cu-BTC synthesized in SS1	1709	1183	1245	1376-1630	3100-3600
Cu-BTC synthesized in SS2	1713	1188		1376-1630	3100-3600

The phase structure of the Cu-BTCs synthesized in SS1 and SS2 was shown in figure 4. Comparing the results with data from the literature (table 2),[20,41] it can be concluded that the Cu-BTC synthesized in SS1 is a mixture of 1D structure catena-triaqua μ - [1,3,5-benzenetricarboxylato]-copper(II) corresponding to the formula $[Cu(BTC)(H_2O)_3]_n$ and micropillar structure $Cu(BTC).3H_2O$.[20,37,41] This will be confimed by the SEM result below. The characteristic peaks of the 1D structure Cu-BTC were displayed at 2θ: 9.2°; 9.9°; 10.9° and 13.5°. Meanwhile, the Cu-BTC synthesized in SS2 has a 3D structure with 2θ: 6.7°; 9.5°; 11.6°; 13.5°. It is known that the formation of 1D or 3D structure Cu-BTC depends on the deprotonation ability of H_3BTC. If the deprotonation is complete, Cu^{2+} ions can react with the 3 carboxylate groups, and the 3D structure Cu-BTC can be obtained. In the case where only partial deprotonation occurs, Cu^{2+} ions only react with two instead of three $–COO^-$ groups and a zigzag structure (1D) is observed.[20] This result can be explained by the fact that $C_2H_5^+$ can push electrons to O-H stronger than CH_3^+ (or the Inductive effect +I of $C_2H_5^+$ is stronger than CH_3^+) leading to the nucleophilic property of OH^- in ethanol is more than OH^- in methanol. This property makes H_3BTC deprotonate totally in ethanol.

Table 2: The position of diffraction peaks of CuBTC synthesized by the potentiodynamic method in SS1 and SS2 compared to the CuBTC from the literature

$Cu(BTC)(H_2O)_3$ 1D[20]	9.3	10.0	11.0		13.4			17.1	18.6		21.4	22.1		24.5
$Cu(BTC).3H_2O$ [41]				11.4		14.0	16.4	17.1	18.8	19.5	21.4	21.7	22.9	24.6
SS1	9.2	9.9	10.9	11.31	13.5		16.13	17.0	18.6	19.46	21.3	22.0	22.8	24.3
$Cu_3(BTC)_2$[20]	*6.8*	*9.6*	*11.8*	*13.6*	*14.9*	*15.2*	*16.7*	*17.7*	*19.2*	*20.5*	*21.5*	*23.1*	*23.5*	*24.2*
SS2	*6.7*	*9.5*	*11.6*	*13.5*	*14.6*	*15.0*	*16.5*	*17.5*	*19.0*	*20.2*	*21.2*		*23.3*	*24.1*

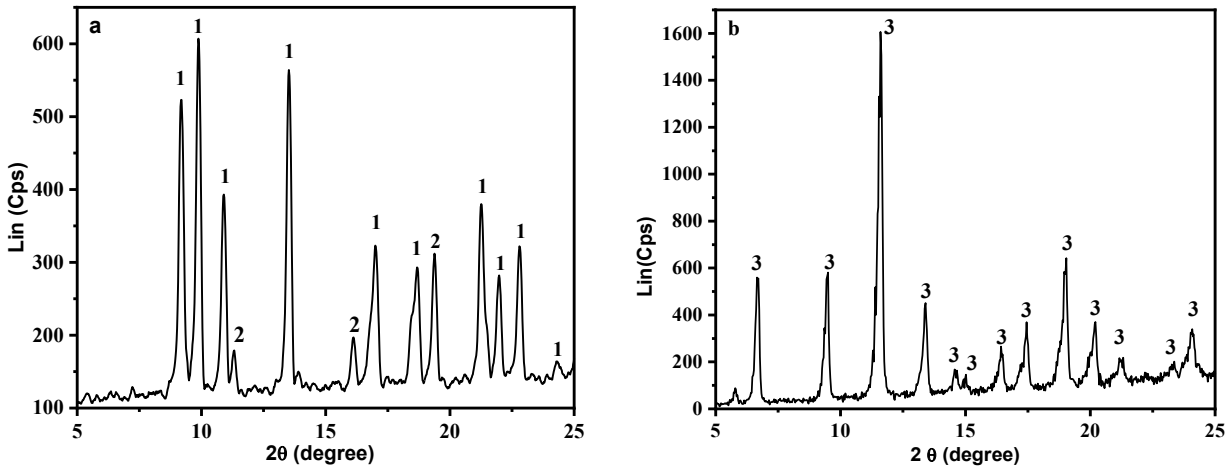

Figure 4: Xray diffraction patterns of Cu-BTC synthesized potentiodynamically in SS1 (a) and SS2 (b). Characteristic peaks: 1 = $[CuBTC(H_2O)_3]_n$ 1D, 2 = $CuBTC.3H_2O$, 3 = $Cu_3(BTC)_2$ 3D

From the 2θ value, (hkl), the distance between crystal plane *d*, the lattice parameter *a* = 26.454 Å of Cu-BTC 3D was calculated, which is similar with the previous result of Wojciech Starosta *et al*. (26.346 Å).[38]

Figure 5 presents the SEM images of the Cu-BTC synthesized in SS1 (a) and SS2 (b). In SS1 with methanol, the obtained Cu-BTC crystals have a size that varies in a large range, from small particles with a size of about 1 µm to a plate shape of about 20 µm. The image is satisfied with the XRD data. In the case of SS2 with ethanol, the Cu-BTC has a cubic shape with sizes ranging from 50 to 500 nm, suitable ith the XRD data above.

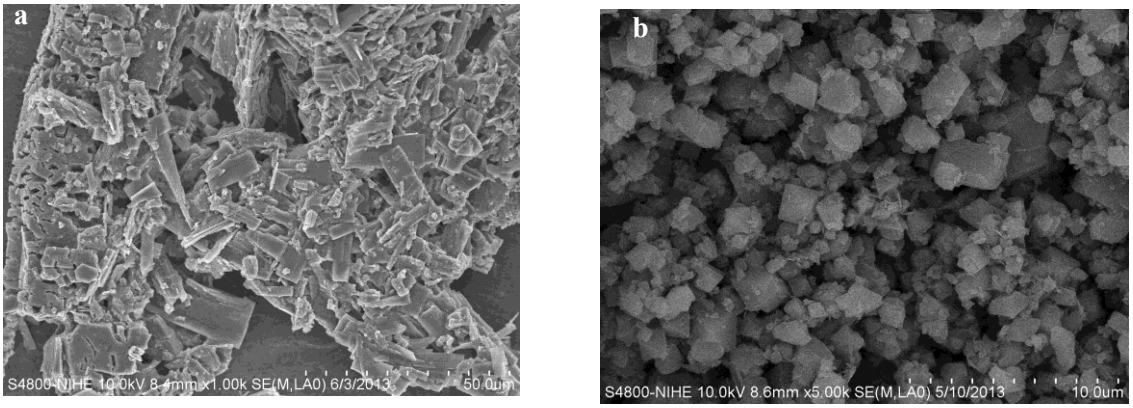

Figure 5: SEM images of Cu-BTC synthesized in SS1 (a) and SS2 (b)

Figure 6 presents the adsorption isotherms in the range p/p_o from 0 to 0.99 at 77 K. While the 1D structure Cu-BTC's isotherms followed type I in the IUPAC classification, which indicated a non-porous structure, the isotherms of the 3D structure Cu-BTC were much closer to a type IV, indicating a highly porous material. A large-range hysteresis loop was also observed, suggesting the presence of bottleneck pores in the 3D structure Cu-BTC. This structure is well suited for the easy capture of CO_2 molecules during adsorption. As expected, the total specific surface area and total pore volume, determined from the BET method, of the 1D structure Cu-BTC were much smaller than that of the 3D structure Cu-BTC (table 3). The micropore volume of the 1D and 3D structure Cu-BTC was 0.01 cm^3/g and 0.25 cm^3/g, respectively. It can be confirmed that the 3D structure Cu-BTC is mainly made of porous structures, which is favorable for CO_2 adsorption.[4,42]

3.2. CO_2 adsorption capacity

Based on the results of the properties of the two synthesized materials, the 3D-structure Cu-BTC was selected for further CO_2 adsorption experiments. The optimum CO_2 uptake (expressed in mass percentage) of material (200 mg) was determined using the Macro-TGA at 25°C and 100% CO_2 (figure 7). It can be observed that the maximum CO_2 uptake reached 3.6 mmol/g which was calculated by the following

formula:

$$Q_{max} = \frac{uptake \times 1000}{M_{CO_2}} = \frac{15.8\% \times 1000}{44} = 3.6\ (\text{mmol.g}^{-1})$$

The presence of micropores in the 3D-structure Cu-BTC could be responsible for this CO_2 uptake. Previous research also highlighted the importance of the specific surface area of the material, especially the microporous structures, on the CO_2 adsorption capacity of the material.[43,44]

Table 3: Specific surface area and pore volume of CuBTC

Material	S_{Total} (m^2/g)	V_{Total} (cm^3/g)	V_{Micro} (cm^3/g)	$d_{Mean\ pore}$ (nm)
1D Cu-BTC	21	0.01	0.01	78.22
3D Cu-BTC	620	0.52	0.25	3.37

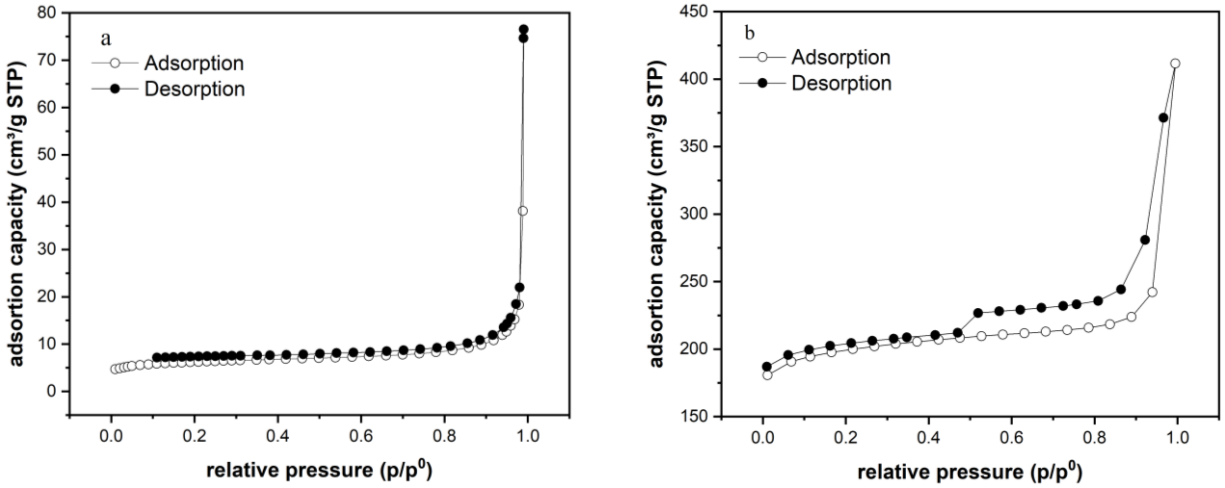

Figure 6: Adsorption isotherms of Cu-BTC synthesized in SS1 (a) and SS2 (b)

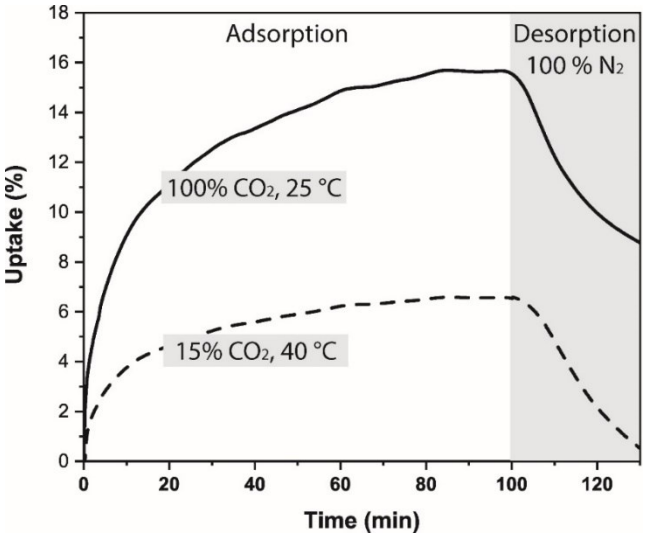

Figure 7: CO_2 uptake of 3D-structure Cu-BTC

To better evaluate the CO_2 adsorption performance of the 3D-structure Cu-BTC, the above result was compared with those of other common CO_2 adsorption materials, such as biomass-derived activated carbons, MOFs, and zeolites (table 4). Most of the CO_2 uptakes of common CO_2 adsorption materials are found in between 2 and 4 mmol/g. Thus, the 3D-structure Cu-BTC synthesized in our research reached a good adsorption capacity, which is in the upper range when comparing with some other materials. It should also be noted that some materials are made from quite complex activation processes and are usually quite time-consuming. This makes it relatively difficult to upcle the production process. These comparative results imply that the use of a simple and quick process as potentiodynamic method to produce the 3D-structure Cu-BTC brings some unique advantages in practical conditions.

The CO_2 uptake of the 3D-structure Cu-BTC was also tested in closer practical conditions, taking into account the diffusion limitation within the bed of sorbent, higher working temperature, and low CO_2 concentration in flue gases. Hence, a bed of 2-cm material (about 2g in mass) was tested for CO_2 adsorption at 40 °C and 15% CO_2 concentration (in N_2). The result (figure 7) showed a significant decrease in the amount of CO_2 uptake, at only 1.3 mmol/g. It can be explained by the fact that high temperatures and low CO_2 concentrations are not favored for physical adsorption is the main adsorption mechanism. Nevertheless, the CO_2 uptake is still reasonable even at high temperatures, and can be

comparable with common adsorbents used in the industry, e.g. hydrotalcites.[49] A small test for cyclic adsorption/desorption was also performed for the 3D-structure Cu-BTC at 25 °C and 100 % CO_2. When a maximum mass was observed, the CO_2 flow was stopped and the N_2 flow was established to regenerate the sample. This protocol was repeated for 5 times. The results showed that the material still achieved a stable CO_2 uptake, suggesting a promising possibility to reuse the material.

Table 4: CO_2 uptake of CuBTC and some other materials

Group	Material	Production condition	CO_2 uptake (mmol g^{-1})
	3D CuBTC (this study)	Synthesized by potentiodynamic procedure	3.60
Biochar/ Activated carbon	Pomegranate peels[43]	Activated by KOH, ratio 1:1 at 700 °C	4.11
	Carrot peels[43]		4.18
	Fern leaves[43]		4.12
	Empty fruit punch[44]	Activated by KOH, ratio 1:5 at 600 °C	1.12
		Activated by KOH, ratio 1:5 at 800°C	2.63
		Hydrothermal at 150, 250, and 350 °C then activated by KOH, ratio 1:5 at 800 °C	3.40 – 3.71 – 2.18
	Olive stone[45]	Activated by CO_2 at 800 °C during 1h, 2h, 4h, 6h and 8h	2.5 – 2.7 – 2.9 – 3.1 – 3.1
	Coffee Ground[46]	Pyrolyzed at 600 °C during 4h, then activated by KOH at 800 °C with ratios 1:1, 1:2, 1:3, and 1:4	3.36 – 3.82 – 3.48 – 3.73
		Pyrolyszed at 600 °C during 4h then activated by KOH, ratio 1:2 at 700, 800 and 900 °C	2.42 – 3.82 – 2.62
Zeolite	Zeolite 13X[47]	Physical impregnation of amine (PEI) on different zeolites	0.36
	Zeolite 13X-MEA[47]		0.45
	Zeolite Meso-13X-PEI_{800MW}[47]		1.32
	Zeolite 13X-$PEI_{600000MW}$[47]		1.22
	Zeolite SBA-$PEI_{750000MW}$[47]		2.15
	Zeolite MCM41-PEI[47]		2.55
Metal-organic framework	MOF UiO-66-NH_2[48]	Different MOF chemically synthesized	3.0
	MOF Cu-BTTr[48]		3.2
	UiO-66-AD8[48]		3.3
	IRMOF-74-III-CH_2NH_2[48]		3.3
	SNU-100-Li[48]		3.4
	SUMOF-3[48]		3.4
	LIFM-33[48]		3.4

4. CONCLUSION

The Cu-BTCs were successfully synthesized by the potentiodynamic method, from 0 to 10 V/SCE at a scan rate of 5 mV/s in the presence of air. The XRD results indicated that the mixture of 1D structure $[Cu(BTC)(H_2O)_3]_n$ and micropillar structure $Cu(BTC).3H_2O$ was obtained when using methanol as a solvent, while the cubic 3D structure Cu-BTC was obtained when using ethanol. With a large total specific surface area obtained, the CuBTC 3D mainly consisted of microporous structures, suitable for CO_2

adsorption. The tests with CO_2 adsorption, both at standard conditions and more realistic conditions confirmed that the 3D structure Cu-BTC could be a potential candidate for CO_2 capture technologies.

Acknowledgements. *The authors gratefully acknowledge the financial support through the bilateral cooperation project between the R.S of Vietnam and Wallonia-Brussels No. 8.2 (2022-2024) and the Vietnam Academy of Science and Technology (VAST), under international mission number QTJP01.02/22-24.*

Conflict of interest. *The authors declare no competing interests.*

REFERENCES

1. J. Zhang, J. Shi, S. Tao, L. Wu, J. Lu. Cu_2O/Ti_3C_2MXene heterojunction photocatalysts for improved CO_2 photocatalytic reduction performance, *Appl. Surf. Sci.*, **2021**, *542*, 148685.
2. M. K. Mondal, H. K. Balsora, P. Varshney. Progress and trends in CO_2 capture/separation technologies: A review, *Energy*, **2012**, *46(1)*, 431-441.
3. F. A. Rahman, M. M. A. Aziz, R. Saidur, W. A. W. A. Bakar, M. R. Hainin, R. Putrajaya, N. A. Hassan. Pollution to solution: Capture and sequestration of carbon dioxide (CO_2) and its utilization as a renewable energy source for a sustainable future, *Renew. Sustain. Energy. Rev.*, **2017**, *71*, 112-126.
4. V. Benedetti, E. Cordioli, F. Patuzzi, M. Baratieri. CO_2 Adsorption study on pure and chemically activated chars derived from commercial biomass gasifiers, *J. CO_2 Util.*, **2019**, *33*, 46-54.
5. H. Yang, S. Orefuwa, A. Goudy. Study of mechanochemical synthesis in the formation of the metal-organic framework $Cu_3(BTC)_2$ for hydrogen storage, *Micropor. Mesopor. Mat.*, **2011**, *143(1)*, 37-45.
6. B. Liu, H. Shioyama, H. Jiang, X. Zhang, Q. Xu. Metal-organic framework (MOF) as a template for synthesis of nanoporous carbons as electrode materials for supercapacitor, *Carbon,* **2010**, *48(2)*, 456-463.
7. B. Liu, X. Zhang, H. Shioyama, T. Mukai, T. Sakai, Q. Xu. Converting cobalt oxide subunits in cobalt metal-organic framework into agglomerated Co_3O_4 nanoparticles as an electrode material for lithium ion battery, *J. Power Sources*, **2010**, *195(3)*, 857-861.
8. S. Marx, W. Kleist, A. Baiker. Synthesis, structural properties, and catalytic behavior of Cu-BTC and mixed-linker Cu-BTC-PyDC in the oxidation of benzene derivatives, *J. Catal.*, **2011**, *281(1)*, 76-87.
9. D. Saha, S. Deng, Z. Yang. Hydrogen adsorption on metal-organic framework (MOF-5) synthesized by DMF approach, *J. Porous Mater.*, **2009**, *16*, 141-149.
10. R. S. Kumar, S. S. Kumar, M. A. Kulandainathan. Highly selective electrochemical reduction of carbon dioxide using Cu based metal organic framework as an electrocatalyst, *Electrochem. Commun.*, **2012**, *25*, 70-73.
11. P. T. S. Nam, P. N. Q. Anh, L. K. A. Ky, P. T. M. Trang. The Knoevenagel reaction using a metal-organic framework (IRMOF-3) as an efficient heterogeneous catalyst, *Vietnam J. Chem.*, **2011**, *49(2ABC)*, 489-496.
12. S. Li, Y. Chen, X. Pei, S. Zhang, X. Feng, J. Zhou, B. Wang. Water Purification: Adsorption over Metal-Organic Frameworks*, Chinese J. Chem.*, **2016**, *34*, 175-185.
13. J. B. DeCoste, G. W. Peterson. Metal-organic frameworks for air purification of toxic chemicals, *Chem. Rev.*, **2014**, *114(11)*, 5695-5727.
14. N. T. Binh, P. T. Thu, N. T. H. Le, D. M. Tien, H. T. Khuyen, L. T. K. Giang, N. T. Huong, T. D. Lam. Study on preparation and properties of a novel photo-catalytic material based on copper-centred metal-organic frameworks (Cu-MOFs) and titanium dioxide, *Int. J. Nanotechnol.*, **2015**, *12(5/6/7)*, 447-455.
15. Q. Rayée, P. T. Nguyen, T. Segato, M.-P. Delplancke-Ogletree, T. Doneux, C. Buess-Herman. Electrochemical synthesis of copper(I) dicyanamide thin films, *J. Electroanal. Chem.*, **2018**, *819*, 331-337.
16. L. T. Hue, N. T. Phuong, D. T. M. Thanh, P. T. T. Ha, N. T. K. Anh. Research on ciprofloxacin adsorption capacity of HKUST-1 synthesized by electrochemical method, *Vietnam J. Sci. Technol.*, **2022**, *60(1)*, 92-104.
17. Y.-K. Seo, G. Hundal, I. T. Jang, Y. K. Hwang, C.-H. Jun, J.-S. Chang. Microwave synthesis of hybrid inorganic-organic materials including porous $Cu_3(BTC)_2$ from Cu(II)-trimesate mixture, *Microporous Mesoporous Mater.*, **2009**, *119(1-3)*, 331-337.
18. S. Kayaert, S. Bajpe, K. Masschaele, E. Breynaert, C. E. A. Kirschhock, J. A. Martens. Direct growth of Keggin polyoxometalates incorporated copper 1,3,5-benzenetricarboxylate metal organic framework films on a copper metal substrate, *Thin Solid Films*, **2011**, *519*, 5437-5440.
19. D. J. Tranchemontagne, J. R. Hunt, O. M. Yaghi. Room temperature synthesis of metal-organic frameworks: MOF-5, MOF-74, MOF-177, MOF-199, and IRMOF-0, *Tetrahedron*, **2008**, *64(36)*, 8553-8557.
20. J. Gascon, S. Aguado, F. Kapteijn. Manufacture of dense coatings of $Cu_3(BTC)_2$ (HKUST-1) on α-

alumina, *Microporous Mesoporous Mater.*, **2008**, *113(1-3)*, 132-138.
21. A. M. Joaristi, J. Juan-Alcañiz, P. Serra-Crespo, F. Kapteijn, J. Gascon. Electrochemical Synthesis of Some Archetypical Zn^{2+}, Cu^{2+}, and Al^{3+} Metal Organic Frameworks*, Cryst. Growth Des.*, **2012**, *12(7)*, 3489-3498.
22. R. Ameloot, L. Stappers, J. Fransaer, L. Alaerts, B. F. Sels, D. E. D. Vos. Patterned Growth of Metal-Organic Framework Coatings by Electrochemical Synthesis, *Chem. Mater.*, **2009**, *21(13)*, 2580-2582.
23. T. R. C. V. Assche, G. Desmet, R. Ameloot, D. E. D. Vos, H. Terryn, J. F. M. Denayer. Electrochemical synthesis of thin HKUST-1 layers on copper mesh, *Microporous Mesoporous Mater.*, **2012**, *158*, 209-213.
24. T. P. Nguyen, T. N. Pham, C. Buess-Herman, T. T. Nguyen, T. M. T. Dinh. Electrochemical synthesis of a metal organic framework material based on copper and benzene-1,3,5-tricarboxylic acid using applied current, *Malaysian J. Chemistry*, **2016**, *18(1)*, 9-26.
25. Y.-R. Lee, J. Kim, W.-S. Ahn. Synthesis of metal-organic frameworks: A mini review, *Korean J. Chem. Eng.*, **2013**, *30*, 1667-1680.
26. P. T. Nguyen, T. T. Nguyen, N. T. Pham, C. Buess-Herman, H. T. L Nguyen, T. T. M. Dinh. Electrosynthesis and characterization of copper dicyanamide materials, *Thin Solid Films*, **2022**, *741*, 138998.
27. H. Al-Kutubi, J. Gascon, E. J. R. Sudholter, L. Rassaei. Electrosynthesis of metal-organic frameworks: challenges and opportunities, *ChemElectroChem*, **2015**, *2*, 462-474.
28. Q. Fang, J. Sculley, H.-C. J. Zhou, G. Zhu. 5.01. Porous Metal-Organic Frameworks, *Comprehensive Nanoscience and technology*, ISBN: 978-0-12-374396-1.
29. N. T. Phuong, C. Buess-Herman, P. T. Nam, N. T. Thom, D. T. M. Thanh. The synthesis of metal organic framework based on Cu, acid benzene-1,3,5-tricarboxylic (H_3BTC) and sodium dicyanamide ($NaDCA\text{-}NaC_2N_3$) using the applied potential method, *Journal of Science of HNUE, Chemical and Biological Sci.*, **2015**, *60(9)*, 59-68.
30. N. T. Phuong, C. Buess-Herman, N. T. Thom, P. T. Nam, T. D. Lam, D. T. M. Thanh. Synthesis Cu-BTC, from Cu and benzene-1,3,5-tricarboxylic acid (H_3BTC) by green electrochemical method, *Green Process. Synth.*, **2016**, *5*, 537-547.
31. U. Mueller, M. Schubert, F. Teich, H. Puetter, K. Schierle-Arndt, J. Pastre´. Metal-organic frameworks-prospective industrial applications, *J. Mater. Chem.*, **2006**, *16*, 626-636.
32. S. S.-Y. Chui, S. M.-F. Lo, J. P. H. Charmant, A. G. Orpen, I. D. Williams. A chemically functionalizable nanoporous material $[Cu_3(TMA)_2(H_2O)_3]_n$, *Science*, **1999**, *283,* 1148-1150.
33. P. Schäfer, A. Lalitha, P. Sebastian, S. K. Meena, J. Feliu, M. Sulpizi, M. A. van der Veen, K. F. Domke. Trimesic acid on Cu in ethanol: Potential-dependent transition from 2-D adsorbate to 3-D metal-organic framework, *J. Electroanal. Chem.*, **2017**, *793*, 226-234.
34. T. Xu, L. Fan, Z. Jiang, P. Zhou, Z. Li, H. Lu, Y. He. Immobilization of N-oxide functionality into NbO-type MOFs for significantly enhanced C_2H_2/CH_4 and CO_2/CH_4 separations, *Dalton Trans.*, **2020**, *49*, 7174-7181.
35. Z. Jiang, Y. Zou, T. Xu, L. Fan, P. Zhou, Y. He. A hydrostable cage-based MOF with open metal sites and Lewis basic sites immobilized in the pore surface for efficient separation and purification of natural gas and C_2H_2, *Dalton Trans.*, **2020**, *49*, 3553-3561.
36. T. Xu, Z. Jiang, P. Liu, H. Chen, X. Lan, D.-L. Chen, L. Li, Y. He. Immobilization of oxygen atoms in the pores of microporous metal-organic frameworks for C_2H_2 separation and purification, *ACS Apply. Nano Mater.*, **2020**, *3(3)*, 2911-2919.
37. R. Pech, J. Pickardt. Catena-Triaqua-μ-[1,3,5-benzenetricarboxylato(2-)]-copper(II), *Acta Cryst.*, **1988**, *C44(6)*, 992-994.
38. W. Starosta, B. Sartowska, K. Łyczko, J. Maurin, A. Pawlukojć, L. Waliś, M. Buczkowski. A method for production of nano MOF and preliminary characterization by selected analytical techniques, *NUKLEONIKA*, **2012**, *57(4)*, 581-583.
39. N. T. L. Lien, N. T. Tung, N. D. Khoa, P. T. S. Nam. Metal-organic framework MOF-199 as an efficient heterogeneous catalyst for the aza-Michael reaction, *Appl. Catal. A: Gen.*, **2012**, *425-426*, 44-52.
40. R. S. Kumar, S. S. Kumar, M. A. Kulandainathan. Efficient electrosynthesis of highly active $Cu_3(BTC)_2$-MOF and its catalytic application to chemical reduction*, Microporous Mesoporous Mater.*, **2013**, *168*, 57-64.
41. A. Kojtari, H.-F. Ji. Metal organic framework micro/nanopillars of $Cu(BTC).3H_2O$ and Zn(ADC).DMSO, *Nanomaterials*, **2015**, *5(2)*, 565-567.
42. V. K. Singh, E. A. Kumar. Comparative Studies on CO_2 Adsorption Kinetics by Solid Adsorbents, *Energy Procedia*, **2016**, *90*, 316-325.
43. J. Serafin, U. Narkiewicz, A. W. Morawski, R. J. Wróbel, B. Michalkiewicz. Highly microporous activated carbons from biomass for CO_2 capture and effective micropores at different conditions, *J. CO_2 Util.*, **2017**, *18*, 73-79.
44. G. K. Parshetti, S. Chowdhury, R. Balasubramanian. Biomass derived low-cost microporous adsorbents for efficient CO_2 capture, *Fuel*, **2015**, *148*, 246-254.

45. A. S. González, M. G. Plaza, F Rubiera, C. Pevida. Sustainable biomass-based carbon adsorbents for post-combustion CO_2 capture, *Chem. Eng. J.*, **2013**, *230*, 456-465.
46. H. Wang, X. Li, Z. Cui, Z. Fu, L. Yang, G. Liu, M. Li. Coffee grounds derived N enriched microporous activated carbons: Efficient adsorbent for post-combustion CO_2 capture and conversion, *J. Colloid Interface Sci.*, **2020**, *578*, 491-499.
47. S. Karka, S. Kodukula, S. V. Nandury, U. Pal. Polyethylenimine-Modified Zeolite 13X for CO_2 Capture: Adsorption and Kinetic Studies, *ACS Omega*, **2019**, *4(15)*, 16441-16449.
48. C. Pettinari, A. Tombesi. Metal-organic frameworks for carbon dioxide capture, *MRS Energy Sustain.*, **2020**, *7*, E35.
49. J. R. McDonough, R. Law, D. A. Reay, V. Zivkovic. Intensified carbon capture using adsorption: Heat transfer challenges and potential solutions, *Therm Sci Eng Prog.*, **2018**, *8*, 17-30.

Corresponding authors: **Nguyen Hong Nam**
University of Science and Technology of Hanoi
Vietnam Academy of Science and Technology
18 Hoang Quoc Viet, Cau Giay, Hanoi 10000, Viet Nam
E-mail: nguyen-hong.nam@usth.edu.vn.

Dinh Thi Mai Thanh
University of Science and Technology of Hanoi
Vietnam Academy of Science and Technology
18 Hoang Quoc Viet, Cau Giay, Hanoi 10000, Viet Nam
E-mail: dtmthanh@itt.vast.vn / dinh-thi-mai.thanh@usth.edu.vn.

